

Image Registration Using PC-Sift-Firefly Optimization

Neha Arora¹, Akhilesh Bhardwaj²

¹M.Tech Scholar, SKIET Kurushetra

²Assistant Professor, SKIET Kurushetra

ABSTRACT: The primary contribution of this research is the development of computational frameworks that tackle in a general and principled way the problems arising in the construction of an image registration system. Specifically, we present a general theory to detect image point features that are suitable for matching. Our theory generalizes and extends much of the previous work on detecting feature locations. A novel algorithm for image features matching is used in terms of evolutionary algorithms. We have efficiently used the firefly optimization to match image features by tuning the rotational angle of image. The complete work is divided into three modules: edge detection, features extraction and features matching. After studying previous work on this, we used the effective phase congruency for the edge detection purpose which removes non uniform illumination problem faced in detection of edges. The requirement of features extraction is that matching points such be which don't change after rotation of image. So we used scale invariant features transform (SIFT) method to extract features and finally we purposed the unsupervised matching algorithm which can work for each type of image. Our features matching using firefly optimizes the rotational angle of test image so that it can best align with the reference image.

KEYWORD: Image Registration, PC-Sift-Firefly Optimization

I. INTRODUCTION

Image registration is the process of finding an optimal geometric transformation between corresponding image data. In other words, given a reference or model, image A, and a test, or floating image, image B, find a suitable transformation, T, such that the transformed test image becomes similar to the reference. The image registration problem typically occurs when two images represent essentially the same object, but there is no direct spatial correspondence between them. The images might be acquired with different sensors, or the same sensor at different times or from different perspectives.

One of the reasons that image registration is an extremely challenging problem is the large degree of variability of the input data. The images that are to be registered and mosaicked may contain visual information belonging to very different domains and can undergo many geometric and photometric distortions such as scaling, rotations, projective transformations, non rigid perturbations of the scene structure, temporal variations, and photometric changes due to different acquisition modalities and lighting conditions. Figure 1.1 shows some examples of image pairs belonging to different domains that have been registered using the algorithms that will be described and analyzed in the next chapters. Despite the large number of efforts made to construct efficient algorithms to solve different aspects of the image registration and mosaicking problem, there still exist a number of obstacles that need to be overcome and several open questions that need to be answered.

Image registration shows up in a rich range of application domains, such as medical image analysis (e.g. diagnosis),

neuroscience (e.g. brain mapping), computer vision (e.g. stereo image matching for shape recovery), astrophysics (e.g. the alignment of images from different frequencies), military applications (e.g. target recognition), etc. Image registration can serve as a powerful tool to investigate how regional anatomy is altered in disease, with age, gender, handedness, and other clinical or genetic factors. One of the most obvious clinical applications of registration is the area of serial imaging. Comparison of scans from a given patient acquired over various time intervals can be routinely performed to follow disease progression, response to treatment and even dynamic patterns of structure change during organ development. Unfortunately, diagnostic imaging scans are not routinely registered in most radiology department; in contrast, the common practice for an examiner is to do one's best to look at film montages of slices that do not match and try to access disease changes. For gross changes this method of comparison may be adequate. For subtle changes, visual comparison of unmatched images is not enough. Image registration can also fuse information from multiple imaging devices to correlate different measures of brain structures and function. Integration of functional and anatomical imaging provides complementary information not available from independent analysis of each modality. Registered high-resolution anatomy in magnetic resonance imaging (MRI), ultrasound (US), or computed tomography (CT) images provides a much more precise anatomical basis for the interpretation of functional and pathologic image data, like single photon emission computed tomography (SPECT), positron emission tomography (PET), and functional MRI

(fMRI). Without registration, the observed activity would be less accurately mapped to the corresponding anatomical structures. Most importantly, intermodality registration can aid interpretation of clinical imaging for critically important treatment decisions.

The overview of image registration is shown in figure 1.2.

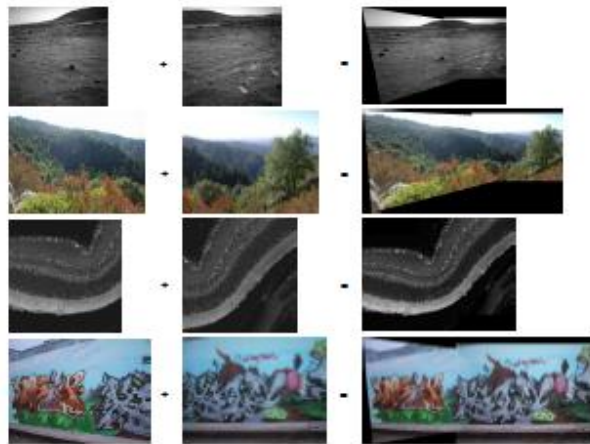


Figure 1.1: Some examples of image pairs that have been registered and mosaicked using the methods. First row: a pair of EDR (extreme dynamic range) images acquired by the right navigation camera of the Spirit rover during its mission to Gusev crater on Mars. Second row: an image pair of a complex 3D outdoor scene taken with a consumer camera. Third row: a pair of retinal images acquired using a confocal microscope. Fourth row: two images of a graffiti scene subject to a strong perspective distortion taken using a consumer camera.

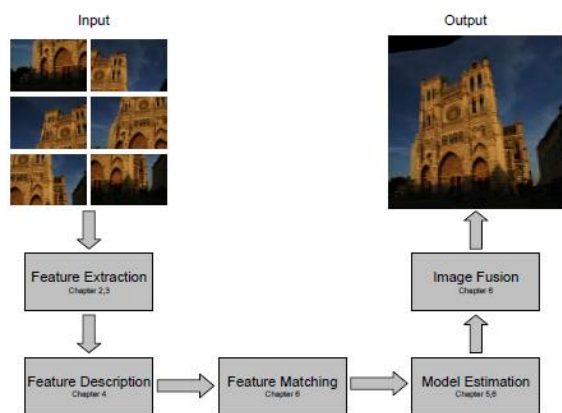


Figure 1.2: Overview of Image registration process

II. PROPOSED WORK

As discussed above our work is related to features matching of two images, of which one image is rotated with some angle to get another image. Then using phase congruency (PC) and shift invariant feature transform (SIFT), both images features are extracted and firefly optimization which is an evolutionary optimization technique is used to match both features. These matched features are shown on both images in next chapter. The whole process can be

categorized into three steps: in the very first we will take out edges in the image. In the second step features in the output image of first step are taken out. These features must be shift invariant i.e. these should be in images even if image is rotated or shifted by some angle. Shift invariant features transformation (SIFT) is used for this. Last step is the important step which is a bio optimized evolutionary algorithm, firefly optimization is used in this step which will match features in respect of minimizing of normalized mean square error.

Phase Congruency

The edge detection in test image is done using PC algorithm which performs well over widely used canny edge detection doesn't perform well in case of non uniform illuminated image. The mathematical formulation of 2-D image PC for our work is given as:

first step is to convolve the normalized iris image $I(x,y)$ with a bank of 2D log-Gabor filters with different orientations and scales. The Log-Gabor has a transfer function of the following form:

$$G(\omega) = \exp\left\{-\frac{(\log(\omega/\omega_0))^2}{2(\log(k/\omega_0))^2}\right\}$$

where ω_0 is the filter's center frequency. k/ω_0 should be a constant for vary ω_0 . The 2D log-Gabor is constructed with the cross-section of the transfer function in the angular direction being a Gaussian function:

$$G(\theta) = \exp\left\{-\frac{(\theta - \theta_0)^2}{2\sigma_\theta^2}\right\}$$

where θ_0 represents the orientation of the filter, σ_θ is the standard deviation of this Gaussian function. Here we choose 6 orientations and 4 scales. Let M_{so}^{even} and M_{so}^{odd} denote the even-symmetric and odd symmetric filter at scale s and orientation o . The response vector can be got by:

$[e_{so}(x,y), o_{so}(x,y)] = [I(x,y) * M_{so}^{even}, I(x,y) * M_{so}^{odd}]$
The amplitude of the response at a given scale and orientation can be computed by:

$$A_{so} = \sqrt{e_{so}(x,y)^2 + o_{so}(x,y)^2}$$

And the phase angle is:

$$\phi_{so}(x,y) = a \tan\left(\frac{o_{so}(x,y)}{e_{so}(x,y)}\right)$$

Let $\bar{\phi}_{so}(x,y)$, denotes the mean phase angle at orientation o , it can be estimated by:

$$\bar{\phi}_0^{even}(x,y), \bar{\phi}_0^{odd}(x,y) = \frac{(\sum_s e_{so}(x,y), \sum_s o_{so}(x,y))}{\sqrt{\sum_s e_{so}(x,y)^2 + \sum_s o_{so}(x,y)^2}}$$

A sensitive phase deviation measure $\Delta\phi_{so}(x,y)$, is used.

$$\Delta\phi_{so}(x,y) = \cos\left(\phi_{so}(x,y) - \bar{\phi}_0(x,y)\right) - \left|\sin\left(\phi_{so}(x,y) - \bar{\phi}_0(x,y)\right)\right|$$

Then the 2D phase congruency is calculated as follows:

$$PC_0(x,y) = \frac{\sum_o \sum_s A_{so}(x,y) (\Delta\phi_{so}(x,y))}{\sum_o \sum_s A_{so}(x,y) + \epsilon}$$

ϵ is a very small positive real number, used to prevent division of zero, its value set to be 0.0001. According to Kovessy, using the magnitude of dot and cross products, the

phase deviation can be calculated directly from the filter outputs, as:

$$\begin{aligned}
 A_{so}(x, y)\Delta\phi_{so}(x, y) &= A_{so}(x, y) \cos(\phi_{so}(x, y) - \bar{\phi}_0(x, y)) \\
 &\quad - \left| \sin(\phi_{so}(x, y) - \bar{\phi}_0(x, y)) \right| \\
 &= (e_{so}(x, y) \cdot \bar{\phi}_0^{even}(x, y) \\
 &\quad + o_{so}(x, y) \cdot \bar{\phi}_0^{odd}(x, y)) \\
 &\quad - (e_{so}(x, y) \cdot \bar{\phi}_0^{odd}(x, y) \\
 &\quad + o_{so}(x, y) \cdot \bar{\phi}_0^{even}(x, y))
 \end{aligned}$$

By this formula the phase congruency of image is calculated.

SIFT

The fundamental work on the SIFT descriptor is presented in the scientific paper by David G. Lowe (Lowe [2004]). This paper describes image features that have many properties that make them suitable for matching differing images of an object or scene. The features are invariant to image scaling and rotation, and partially invariant to change in illumination and 3D camera viewpoint. They are well localized in both the spatial and the frequency domains, reducing the probability of disruption by occlusion, clutter, or noise. Large number of features can be extracted from typical images with efficient algorithms. The SIFT algorithm uses a no of computation stages which are as:

Scale-space extrema detection - first step is to go over all scales and image locations with difference-of-Gaussian function and identify potential scale and orientation invariant interest points. Computed from the difference of two nearby scales separated by a constant multiplicative factor k, scale-space extrema in the difference-of-Gaussian function convolved with the image, $D(x, y, \sigma)$ is used to efficiently detect stable feature point locations in scale space.

$$D(x, y, \sigma) = (G(x, y, \sigma) - G(x, y, \sigma)) * I(x, y) = L(x, y, k\sigma) - L(x, y, \sigma)$$

Key point localization, basing on measures of keypoint stability - as we have a interest point candidate, we proceed to perform a detailed fit to the nearby data for location, scale, and ratio of principal curvatures. This way we reject the points that have low contrast (and are therefore sensitive to noise) or are poorly localized along an edge. Lowe (Lowe [2004]) uses the Taylor expansion (up to the quadratic terms) of the scale-space function, $D(x, y, \sigma)$, shifted so that the origin is at the sample point:

$$D(x) = D + \frac{\partial D^T}{\partial x} x + \frac{1}{2} x^T \frac{\partial^2 D}{\partial x^2} x$$

where D and its derivatives are evaluated at the sample point and $x = (x, y, \sigma)$ T is the offset from this point. The location of the extremum, \hat{x} , is determined by taking the derivative of this function with respect to x and setting it to zero, thus:

$$\hat{x} = - \frac{\partial^2 D^{-1}}{\partial x^2} \frac{\partial D}{\partial x}$$

Orientation Assignment - an invariance to image rotation is achieved by assigning consistent orientation to each keypoint based on local image properties, afterwards the keypoint descriptor is also represented relative to this orientation. The scale of the keypoint is used to select the Gaussian smoother image L with the closest scale, so that all computations are performed in a scale-invariant manner. For each image sample L(x,y) at this scale, the gradient magnitude, $m(x,y)$, and the orientation, $\theta(x,y)$, is pre computed using pixel differences:

$$\begin{aligned}
 m(x, y) &= \sqrt{(L(x+1, y) - L(x-1, y))^2 + (L(x, y+1) - L(x, y-1))^2} \\
 \theta(x, y) &= \tan^{-1} ((L(x+1, y) - L(x-1, y)) / (L(x, y+1) - L(x, y-1)))
 \end{aligned}$$

An orientation histogram is formed from the gradient orientations of sample points within a region around the key point. The orientation histogram has 36 bins covering the 360 degree range of orientations. Each sample added to the histogram is weighted by its gradient magnitude and by a Gaussian-weighted circular window with a σ that is 1.5 times that of the scale of the keypoint. Peaks in the orientation histogram correspond to dominant directions of local gradients. The highest peak in the histogram is detected, and then any other local peak that is within 80% of the highest peak is used to also create a keypoint with that orientation. Therefore, at locations with multiple peaks of similar magnitude, there will be multiple keypoints created at the same location and scale but different orientations (Lowe [2004]).

Key point descriptor - by means of the keypoint scale, the Gaussian blur level of the current image is defined. The gradient magnitudes and orientations are sampled around the keypoint location on the image. Invariance is achieved by rotating the gradient orientations and descriptor coordinates in relation to the orientation of the feature point. A Gaussian weighting function with σ equal to one half the width of the descriptor window is used to assign a weight to the magnitude of each sample point. The purpose of the Gaussian window is to avoid sudden changes in the descriptor with small changes in the position of the window, and to give less emphasis to the gradients that are far from the center of the descriptor, as these are most affected by mis registration errors (Lowe [2004]). The interest point descriptor is shown on Fig. 3.5.

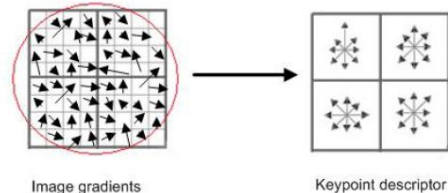


Figure 3.5: A keypoint descriptor is created by first computing the gradient magnitude and orientation at each

image sample point in a region around the key point location, as shown on the left. These are weighted by a Gaussian window, indicated by the overlaid circle. These samples are then accumulated into orientation histograms summarizing the contents over 4x4 sub regions, shown on the right, with the length of each arrow corresponding to the sum of gradient magnitudes near that direction within the region. This figure shows a 2x2 descriptor array computed from a 8x8 set of samples, whereas the experiments in this paper use 4x4 descriptors computed from 16x16 sample array

Feature Matching (Firefly Optimization)

Features mapping have equal importance as above steps. We have used a bio optimized matching algorithm i.e. firefly optimization. The reference image is rotated by some angle just for testing purpose. In firefly optimization, we optimize the optimum angle of rotation of the test image on the basis of minimizing mean square error in features of reference image and test image. The features descriptor obtained from the previous module for reference as well as test image is fed into matching module, so that a minimum difference between them can be reached. The fitness function to be minimized is the mean square error given as:

$$MSE = \frac{\text{sum}(\text{diff}^2)}{\text{size}(\text{features})}$$

For matching firefly algorithm is used as said, it is explained as:

In the firefly algorithm, there are two important points: the variation in the light intensity and formulation of the attractiveness. For simplicity, we can assume that the attractiveness of a firefly is determined by its brightness which in turn is connected with the encoded objective function. In the simplest case for maximum optimization problems, the brightness I of a firefly for a particular location x could be chosen as $I(x) = f(x)$. Even so, the attractiveness β is relative, it should be judged by the other fireflies. Thus, it will differ with the distance r_{ij} between firefly i and firefly j . In addition, light intensity decreases with the distance from its source, and light is also absorbed by the media, so we should allow the attractiveness to vary with the varying degree of absorption. In the simplest form, the light intensity $I(r)$ varies according to the inverse square law.

$$I(r) = \frac{I_0}{r^2} \quad (1)$$

Where I_0 is the intensity at the source. For a stated medium with a fixed light absorption coefficient γ , the light intensity I varies with the distance r . That is

$$I = I_0 e^{-\gamma r}$$

Where I_0 is the initial light intensity, In order to avoid the singularity at $r = 0$ in the expression $\frac{I(r)}{r^2}$, the combined effect of both the inverse square law and absorption can be approximated as the following Gaussian form

$$\beta = \beta_0 e^{-\gamma r^2}$$

Where β_0 is the attractiveness at $r = 0$. Since it is often faster to calculate $1/(1 + \gamma r^2)$ than an exponential function, the above function, if necessary, can be approximated as

$$\beta = \frac{\beta_0}{(1 + \gamma r^2)}$$

In the real time implementation, the attractiveness function $\beta(r)$ can be any monotonically decreasing functions such as the following generalized form

$$\beta(r) = \beta_0 e^{-\gamma r^m}$$

For a fixed, the characteristic length becomes

$$\Gamma = \gamma^{-\frac{1}{m}}$$

Conversely, for a specific length scale Γ in an optimization problem, the parameter γ can be used as a typical initial value. That is

$$\gamma = \frac{1}{\Gamma^m}$$

The distance between any two fireflies i and j at x_i and x_j , respectively is the Cartesian distance.

$$r_{i,j} = \sqrt{\sum_{k=1}^d (x_{i,k} - x_{j,k})^2}$$

The movement of the firefly i is attracted to another more attractive (brighter) firefly j is determined by

$$x_i = x_i + \beta_0 e^{-\gamma r^2} (x_j - x_i) + \alpha \epsilon_i$$

Where the second term is due to the attraction and third term is randomization with α being the randomization parameter, and is a vector of random numbers being drawn from a Gaussian distribution or uniform distribution. For example, the simplest form is ϵ_i could be replaced by $(\text{rand} - \frac{1}{2})$ where rand is a random number generator uniformly distributed in $[0, 1]$. For most of our implementation, we can take $\beta_0 = 1$ and $\alpha \in [0, 1]$.

It is worth pointing out that above equation is a random-walk partial towards the brighter fireflies. If $\beta_0 = 0$, it becomes a simple random walk.

The parameter γ now characterizes the contrast of the attractiveness, and its value is crucially important in determining the speed of the convergence and how the FA algorithm behaves. In theory, $\gamma \in [0, \infty)$, but in actual practice, $\gamma = O(1)$ is determined by the characteristic length Γ of the system to be optimized. Thus, for most applications, it typically varies from 0.1 to 10

III. RESULTS

The work is implemented using MATLAB's image processing toolbox. The reference image is rotated by 20° angle as shown in figure 2.

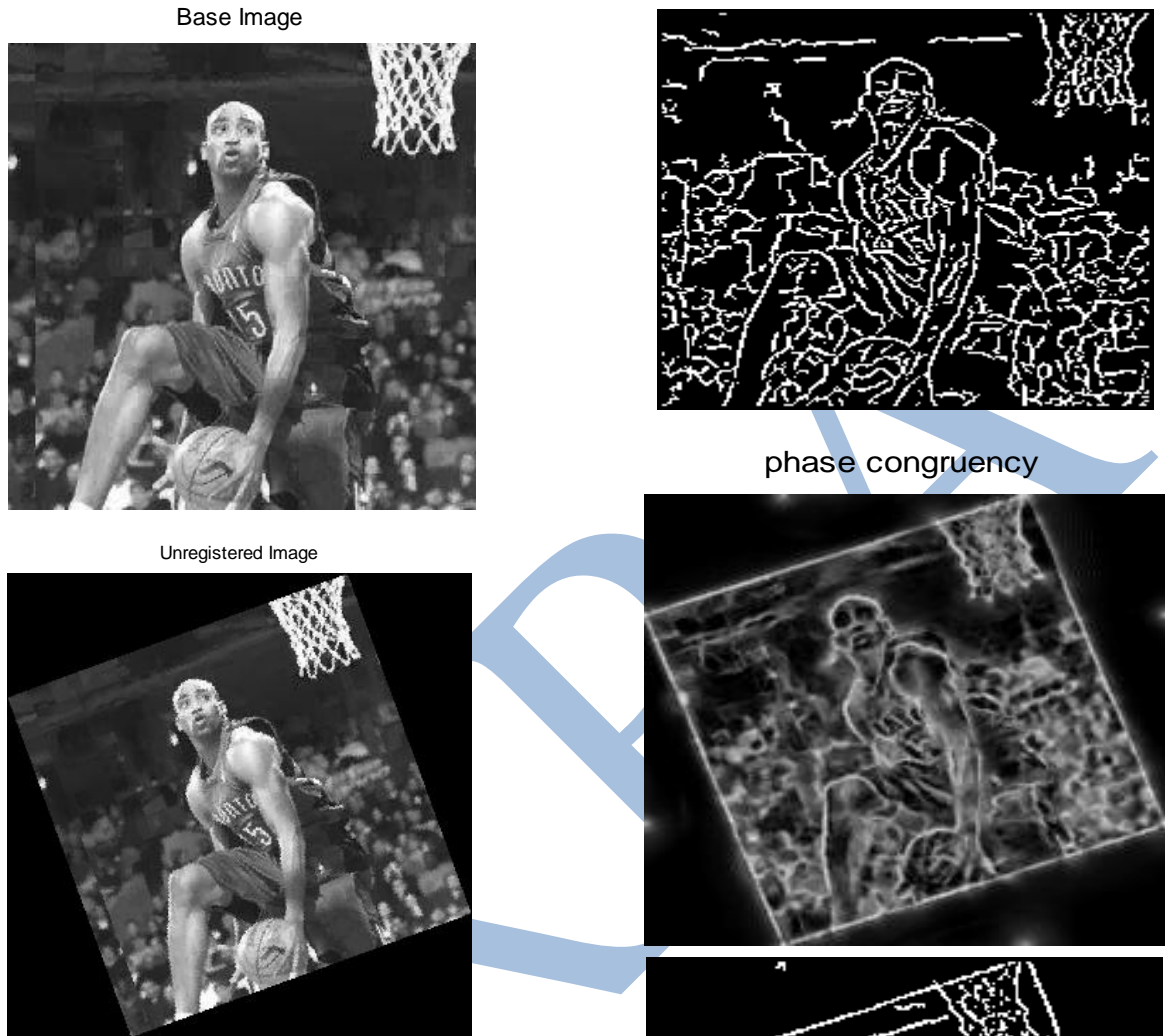


Figure 2: (a) reference image (b) Rotated Image

The phase congruency output for both images is shown in figure 3 below.

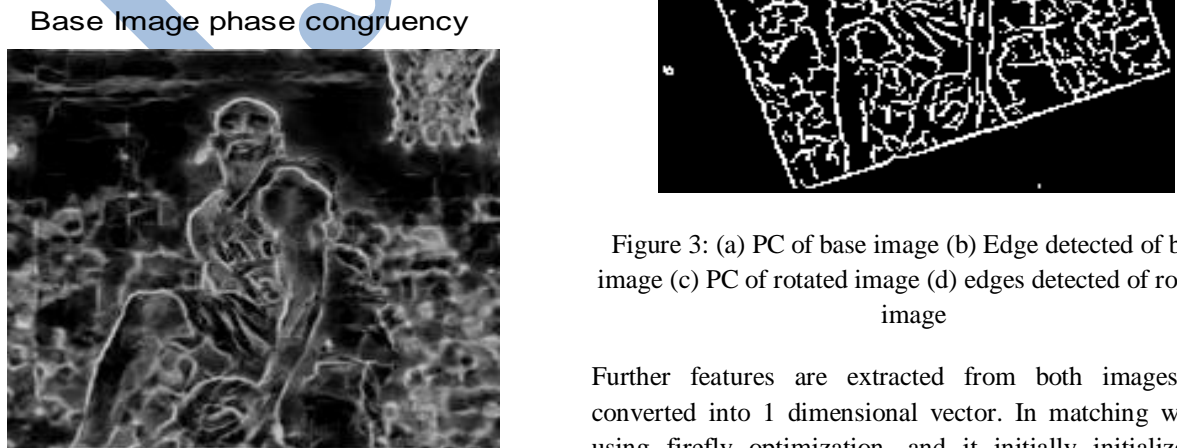


Figure 3: (a) PC of base image (b) Edge detected of base image (c) PC of rotated image (d) edges detected of rotated image

Further features are extracted from both images and converted into 1 dimensional vector. In matching we are using firefly optimization, and it initially initialize the

rotation angle randomly, so results may vary from the results pasted in the file, when executed. We have run the algorithm for 3-4 times for each image and best results are chosen here. After using proposed matching algorithm the features points are matched more than simple matching algorithm whose result is shown in figure 4. Figure 5 shows the points matched in both images after rotating the image by optimized rotation angle and checking out points matching.

The mapping of features is shown in figure 5 and aligned images are shown in figure 6 after making one opaque by 60%. The normalized matching value calculated by number of points at same location for both cases is 0.3589 and 1.0870. Some more images are used for testing and results of them and their matching values are shown in table 1.

Table 1: Normalized image Matching value

Image	Normalized Matching Value	Proposed Normalized Matching Value
NBA player	0.3589	1.0870
pepper	0.3049	0.5634
Beach image	0.4866	0.6720

A comparison for above table shows that for the proposed work, normalized matching value is higher for every type of image.

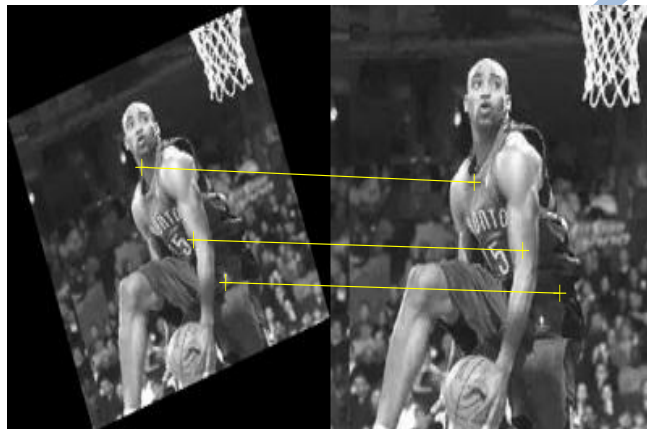


Figure 4: features points matched in both images

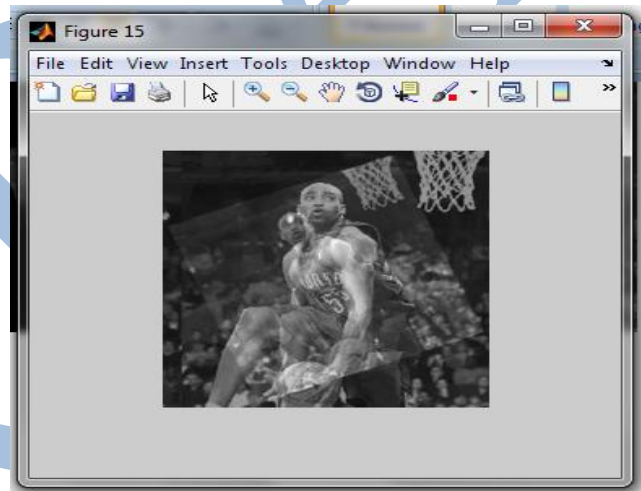


Figure 6: images alignment after making one opaque by 60 %

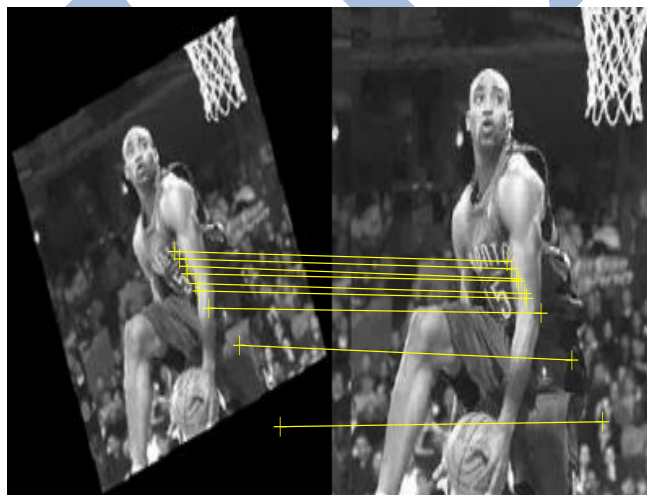


Figure 5: Points matched after proposed work

IV. CONCLUSION

We have used general images for testing purpose but this is a generalized algorithm and can work for any type of input image whether that can be medical or satellite images. Unsupervised learning in the form of firefly algorithm makes it generalize for every type of image. Firefly optimisation is an evolutionary optimization algorithm which changes its firefly's position to move towards a more brighter firefly. In our case it will search for the optimum angle at which matching points between test and reference image are maximum. We considered mean square error between features points location extracted from the module 2 using SIFT. After optimization the rotational angle set to a minimum value for which more number of matching points exist and test image is aligned with the reference image by that optimum angle. The images used here are

compressed to 200*200 so that execution time can be reduced. A comparison of proposed algorithm with without optimization is shown in table 1.

V. References

- [1] Medha V. Wyawahare, "Image Registration Techniques: An overview" International Journal of Signal Processing, Image Processing and Pattern Recognition, Vol. 2, No.3, September 2009.
- [2] Shanmugapriya. S, "An intensity-based medical image Registration using genetic algorithm" Signal & Image Processing : An International Journal (SIPIJ) Vol.5, No.3, June 2014.
- [3] Luiz Satoru Ochi, "Image Registration Using Genetic Algorithms" GECCO'08, July 12-16, 2008.
- [4] Ch.Venkateswara Rao, "OPTIMIZATION OF AUTOMATIC IMAGE REGISTRATION ALGORITHMS AND CHARACTERIZATION"IEEE Trans. On Pattern Anal. And Machine Intell.2008.
- [5] Andrea Valsecchi, "An Image Registration Approach using Genetic Algorithms" IEEE World Congress on Computational Intelligence June, 10-15, 2012.
- [6] Siddharth Saxena, " A Survey of Recent and Classical Image Registration Methods" International Journal of Signal Processing, Image Processing and Pattern Recognition Vol.7, No.4 (2014), pp.167-176.
- [7] Feng Jin, "Image Registration Algorithm Using Mexican Hat Function-Based Operator and Grouped Feature Matching Strategy" e95576. doi:10.1371/journal.pone.0095576, 2014.
- [8] Renbo Xia, "A robust feature-based registration method of multimodal image using phase congruency and coherent point drift" Pattern Recognition and Computer Vision, 2014.
- [9] Peter Kovesei, "Phase Congruency Detects Corners and Edges" Multiple View Geometry in Computer Vision. Cambridge University Press (2000).
- [10] P.Subha, "Automatic Feature Based Image Registration using DWT and SIFT" IJESC, 2014.
- [11] Supriya S. Kothalkar, "Multimodal Image Registration using Contour let Transform" International Journal of Advanced Research in Computer and Communication Engineering, Vol. 3, Issue 3, March 2014.
- [12] Dilipsinh Bheda, "A Study on Features Extraction Techniques for Image Mosaicing" International Journal of Innovative Research in Computer and Communication Engineering ,Vol. 2, Issue 3, March 2014.
- [13] Megha M Pandya , "Accurate Image Registration using SURF Algorithm by Increasing the Matching Points of Images" International Journal of Computer Science and Communication Engineering Volume 2 Issue 1 (February 2013 Issue).
- [14] Rakesh Singhai , "Registration of Satellite Imagery Using Genetic Algorithm" Proceedings of the World Congress on Engineering 2012 Vol II WCE 2012, July 4 - 6, 2012.
- [15] Mahmood Amintoosi, "Image Registration for Super-Resolution using SIFT Key-points"ICEE, 2009.
- [16] Zaafour Ahmed, "Satellite Images features Extraction using Phase Congruency model" IJCSNS International Journal of Computer Science and Network Security, VOL.9 No.2, February 2009.
- [17] Peter J. Myerscough, "ESTIMATING THE PHASE CONGRUENCY OF LOCALISED FREQUENCIES" Journal of Computer Vision Research, 2010.
- [18] Xiaoyan Yuan, "Iris Feature Extraction Using 2D Phase Congruency" Proceedings of the Third International Conference on Information Technology and Applications, 2005.
- [19] J. Krishna Chaithanya, " Feature Extraction of Satellite Images Using 2D Phase Congruency Measure" International Journal of Emerging Technology and Advanced Engineering, Volume 3, Issue 1, January 2013.
- [20] J. Krishna Chaithanya, Dr. T. Rama Shri," Feature Extraction of Satellite Images Using 2D Phase Congruency Measure", International Journal of Emerging Technology and Advanced Engineering, Volume 3, Issue 1, January 2013
- [21] Andriy Myronenko and Xubo Song," Point Set Registration: Coherent Point Drift", IEEE Transactions On Pattern Analysis And Machine Intelligence, VOL. 32, NO. 12, DECEMBER 2010
- [22] Andrea Valsecchi and Sergio Damas," An Image Registration Approach using Genetic Algorithms", IEEE World Congress on Computational Intelligence June, 10-15, 2012 - Brisbane, Australia
- [23] N.NagaRaju, T.Satya savitri, Ch.A.Swamy," Image Registration Using Scale Invariant Feature Transform" International Journal of Scientific Engineering and Technology, Volume No.2, Issue No.7, 2013.
- [24] Haidawati Nasir, Vladimir Stankovic," Image Registration For Super Resolution Using Scale Invariant Feature Transform, Belief Propagation And Random Sampling Consensus", 18th European Signal Processing Conference (EUSIPCO-2010)
- [25] Gao Ting, Xu Yu, and Xu Ting-xin," Multi-Scale Image Registration Algorithm based on Improved SIFT", Journal of Multimedia, Vol. 8, No. 6, December 2013
- [26] Samuel Cheng, Vladimir Stanković and Lina Stanković," IMPROVED SIFT-BASED IMAGE REGISTRATION USING BELIEF PROPAGATION", ICASSP 2009
- [27] M.C. Morrone, J.R. Ross, "Mach bands are phase dependent", Nature, November 1986
- [28] M.C. Morrone, R.A. Owens, 'Feature detection from local energy', Pattern Recognition Letters, 1987
- [29] M.C. Morrone, D.C. Burr, 'feature Detection in human vision: A phase dependent energy model', proc. R. Soc. Lond. B. 1988p.